Effect of temperature on the electron distribution in illuminated heterostructures

C. M. Hurd and S. P. McAlister
Solid State Chemistry, National Research Council of Canada, Ottawa, Canada K1A 0R9

D. J. Day
Bell-Northern Research, P.O. Box 3511, Station C, Ottawa, Canada K1Y 4H7
(Received 20 July 1988; revised manuscript received 3 October 1988)

We solve the 1D Poisson equation for a model heterostructure containing photoexcitable donors and derive solutions for different temperatures in the range 77–300 K. We consider a single-interface GaAs/$Al_xGa_{1-x}As$ heterostructure having deep donors in both the $Al_xGa_{1-x}As$ supply layer and in the GaAs buffer, but our approach is applicable to other configurations. The calculation accounts for photogenerated electrons arising from simulated *DX* centers in the $Al_xGa_{1-x}As$ layer and from impurity donors in the GaAs buffer. Using realistic parameters in a quantitative calculation applicable to steady illumination, we show how light affects the internal distribution of free electrons among the active layers. The results give a transparent picture of the factors that control the response of a unipolar heterostructure to light at different temperatures.

I. INTRODUCTION

High-electron-mobility transistors (HEMTs) based on GaAs/$Al_xGa_{1-x}As$ heterostructures with typically $0.2 \leq x \leq 0.4$ are sensitive to light. This sensitivity arises[1–8] from deep traps located primarily in the $Al_xGa_{1-x}As$ supply layer, although similar traps in the GaAs buffer layer may also contribute.[3] Illumination increases the density of free electrons in the active layers by photoionizing the deep traps. This modifies the macroscopic potential barriers in the structure, leading to a redistribution of the total free charge among the active layers. The internal potential barriers control the access to the conduction channels for electrons passing between source and drain,[9] so these internal access resistances are also affected by illumination.

Shining light on a HEMT produces a complicated set of interacting internal changes. Experiments have shown that they lead to various effects such as a shift in threshold voltages,[1,4] reversal of drain collapse,[1,4] and, at low enough temperatures, persistent photoeffects.[3,5–8] Furthermore, experiments using fixed levels of continuous illumination[10,11] show that the response of a typical supply layer material to a given light intensity depends on temperature; the response increases as temperature is reduced from room temperature. Recent experiments[12] confirm this behavior for a typical $Al_xGa_{1-x}As$ heterostructure.

The effects of illumination on the distribution of charge in a structure have so far been described only qualitatively.[3,6–8] Here we take the description a step further quantitatively by incorporating photoexcitable traps into the standard one-dimensional (1D) Poisson equation. We concentrate on illustrating the effects of temperature on the response to illumination. For the sake of illustration, we consider a typical unipolar heterostructure and, using realistic values for the parameters involved, calculate for different temperatures the potential of the conduction-band edge in the structure in the dark or in steady illumination. Although our approach is restricted to a 1D view, it gives a graphical picture of the factors that control this structure's response to light at different temperatures; it is a first step toward a more quantitative understanding of the experimental effects mentioned above.

We give details of the model in Sec. II, and of the calculation in Sec. III. In Sec. IV we show results for the electron distribution in the dark and illuminated cases for temperatures between 77–300 K. We give a brief summary of our conclusions in Sec. V.

II. MODEL HETEROSTRUCTURE

Figure 1 shows the model structure. We use a conventional configuration with typical dimensions, but our treatment could be applied to other configurations. We assign to each layer an arbitrary density n_s of shallow donors, which are photoinert in this model. These shallow donors, which may represent doping in the cap and supply layers, and unintentional impurities elsewhere, are assumed to be in thermal equilibrium with the conduction bands. We also assign an arbitrary density n_d of deep, photoexcitable donors to the supply and buffer layers. We find it convenient to imagine (Fig. 2) the configuration of donors and conduction bands as in Saxena,[13] but the calculation is independent of the picture adopted to interpret the activation energies involved. For the sake of argument we choose E_s so that $E_{\Gamma s} \equiv E_\Gamma - E_s = 0.01$ eV in all layers (cf. p. 21 of Ref. 14). But we choose different values of E_d in the supply and buffer layers such that at room temperature $E_{Ld} \equiv E_L - E_d = 0.44$ eV in the $Al_{0.3}Ga_{0.7}As$ layer, so that the donor may represent[3] a *DX* center, and $E_{Ld} = 0.80$ eV in the buffer, so that it may represent[3] a typical deep donor in GaAs.

To derive the carrier distribution in the structure we need N_i^+, the total density of ionized donors in the ith

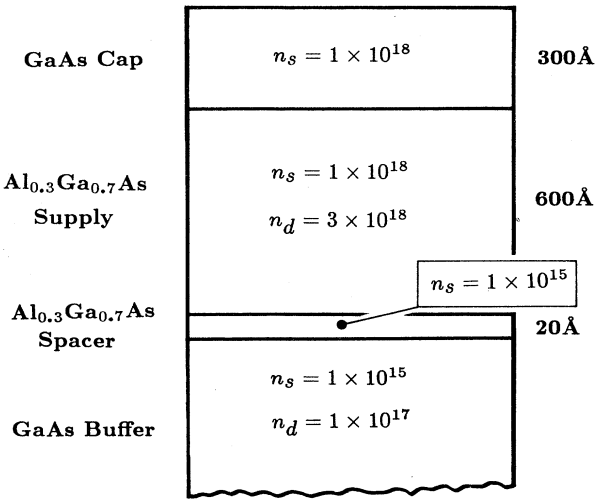

FIG. 1. Model heterostructure used in the calculations. The density n_s of shallow donors, and n_d of deep, is given in cm^{-3}. Deep donors are photoexcitable; shallow ones are photoinert. Deep donors are absent in the cap and spacer. We include a spacer to be realistic, but it has no material effect on the results.

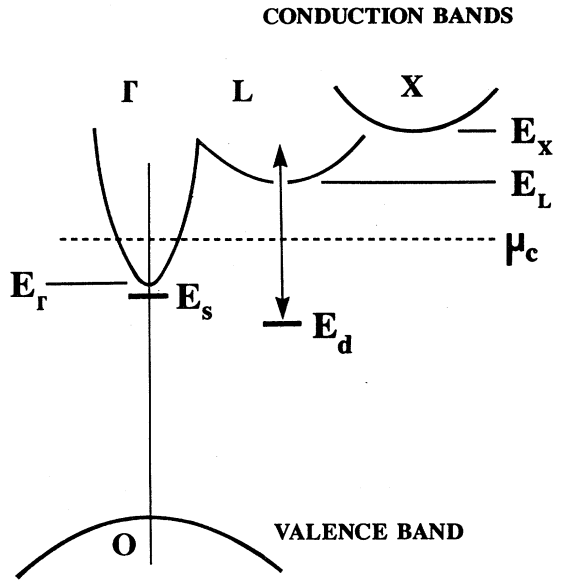

FIG. 2. Relationship of the shallow donor of energy E_s, and the deep E_d, to the conduction bands envisaged for the supply or buffer layers in Fig. 1. The difference $E_\Gamma - E_s$ is set at 0.01 eV in all layers, and at room temperature $E_L - E_d$ is set at 0.44 eV in the supply layer and 0.80 eV in the buffer. μ_c is the quasi-Fermi level of the conduction bands and the shallow donor.

heterolayer. Then we can solve simultaneously the 1D Poisson equation

$$\frac{d^2\phi}{dx^2} = (-q/\epsilon_s)[N_i^+ - n(x)] \tag{1}$$

and the Maxwell-Boltzmann approximation

$$n(x) = D_i \exp[\beta(\phi + \Delta\phi_i)] , \tag{2}$$

where $\phi(x)$ is the variation of the electrostatic potential of the conduction band edge (referred to the Fermi level μ_c of the conduction bands) in the direction x normal to the heterointerface, $n(x)$ is the electron density, $\beta \equiv (1/k_B T)$, and other terms have their usual meanings.[14] For the ith layer, $\Delta\phi_i$ is the conduction-band-edge difference, and D_i is the effective mass density of states of the conduction band, taking into account the multivalley conduction.[10]

To get N_i^+, and to account for illumination, we take the following steps.[15] For a general layer $N_i^+ = n_d^+ + n_s^+$, comprising n_d^+ from the photoexcitable deep donors and n_s^+ from the inert shallow ones. The density of ionized deep donors is

$$n_d^+ = \frac{n_d}{1 + g_d \exp[\beta(\mu_d - E_d)]} , \tag{3}$$

where g_d is the donor degeneracy and μ_d is the quasi-Fermi level of the deep donors. Since the exponential term can be expressed as the product

$$\exp[\beta(E_\Gamma - E_d)]\exp[\beta(\mu_d - \mu_c)]\exp[\beta(\mu_c - E_\Gamma)] ,$$

we can write Eq. (3) as

$$n_d^+ = \frac{n_d}{1 + z_d y} , \tag{4}$$

where $z_d \equiv (g_d/R)\exp(\beta E_{\Gamma d})$, $R \equiv \exp[\beta(\mu_c - \mu_d)]$, and $y \equiv \exp[-\beta(E_\Gamma - \mu_c)]$. In terms of the electrostatic potential of Eq. (2), $y \equiv \exp[-\beta(\phi + \Delta\phi)]$. We also have corresponding to Eq. (4)

$$n_s^+ = \frac{n_s}{1 + z_s y} , \tag{5}$$

where $z_s \equiv g_s \exp(\beta E_{\Gamma s})$.

The effect of illumination is contained entirely in the behavior of μ_d. This we have written in terms of R, which relates[16] the separation of the quasi-Fermi levels in the dark and in the light. It is convenient to go a step further and write R in terms of $\delta\epsilon_n/c_n$, where $\delta\epsilon_n$ is the increase produced in the emission coefficient of the donor by a given level of steady illumination, and c_n is the capture coefficient. One can show[15] that R is related to the fractional increase in the emission coefficient by $R = 1 + (\delta\epsilon_n/\epsilon_n)$ or

$$R = 1 + g_d(\delta\epsilon_n/c_n)_x \exp(\beta E_{Ld}) , \tag{6}$$

where $(\delta\epsilon_n/c_n)_x$ is the value of the illumination parameter at a distance x below the illuminated surface, taking into account optical absorption.

III. CALCULATION

We choose a value of $(\delta\epsilon_n/c_n)_{x=0}$ to represent the intensity of the light incident on the top surface. Although $\delta\epsilon_n/c_n$ is an arbitrary parameter, we know empirically[12] its approximate relationship to the equivalent photon flux

at 660 nm, and we use this to ensure a realistic choice. Throughout the paper we use either $(\delta\epsilon_n/c_n)_{x=0}=0$ for the "dark" condition, or 1×10^{-4} for the "light." The latter corresponds to $\sim1.5\times10^{17}$ photons s^{-1} cm^{-2} at 660 nm.

Then for each layer we derive from standard empirical relationships[17–20] the band factors E_Γ, E_L, E_X, the effective density of states[10] D_i, and the band-edge difference[21] $\Delta\phi_i$. We include for completeness the empirical temperature dependences[17,20] of the band parameters, as explained in Sec. III (C) of Ref. 12. (This is a cosmetic refinement, however, because the effect of these temperature dependences in the calculation is negligible compared to that arising from β.) Since E_d and E_s (Fig. 2) have assigned values (Sec. II), E_{Ld}, $E_{\Gamma s}$, and $E_{\Gamma d}$ can be evaluated leading to $R(x)$ and $N_i^+(x)$. E_d and E_s are defined with respect to E_Γ. Thus $E_{\Gamma s}$ and $E_{\Gamma d}$ are independent of temperature, but E_{Ld} has the small[12] temperature dependence of E_L relative to E_Γ.

We put $g_d=g_s=2$ throughout, and use the same optical absorption coefficient for both GaAs and $Al_{0.3}Ga_{0.7}As$. This is justified by the results of Aspnes *et al.*[22] who find, for example, that for an energy of 1.9 eV ($\sim$650 nm) the absorption coefficient is $\sim3.4\times10^4$ cm^{-1} for GaAs and $\sim2.1\times10^4$ cm^{-1} for $Al_{0.32}Ga_{0.68}As$. It depends strongly on energy. If we use a coefficient of order 10^4 cm^{-1}, however, the effects of absorption are imperceptible on the scale of the following figures. So for the sake of illustrating the effects of temperature when the absorption is appreciable, we use arbitrarily 5×10^5 cm^{-1} throughout. (We have described elsewhere[23] the effects of varying the absorption coefficient at a fixed temperature.) To obtain $n(x)$ and $\phi(x)+\Delta\phi(x)$ we solve Eqs. (1) and (2) iteratively by Gummel's method[24] of first-order linearization, using chosen boundary conditions.[25] Details of this method are given in the Appendix.

IV. RESULTS FOR THE MODEL HETEROSTRUCTURE

A. Effect of light at a fixed temperature

Before considering the effects of temperature on the illuminated structure, it is helpful to look first at the effects of light at a fixed temperature. For the sake of argument, we choose 77 K because the effects are more pronounced there.

Figure 3 shows $n(x)$ and $\phi(x)+\Delta\phi(x)$ of Eq. (2) in the active layers when in the dark or the light. The $Al_{0.3}Ga_{0.7}As$ layer in Fig. 1 is thick enough that is not totally depleted, and $n(x)$ in the dark has a broad maximum of $\sim4.7\times10^{17}$ cm^{-3} flanked by depletion regions, each $\sim1.2\times10^{-6}$ cm wide, and prominent peaks corresponding to the charge trapped in the cap/$Al_{0.3}Ga_{0.7}As$ and the $Al_{0.3}Ga_{0.7}As$/buffer interfaces. Illumination photoionizes the deep donors in both the supply and buffer layers, leading to a reduction in the widths of the depletion regions to $\sim0.55\times10^{-6}$ cm each, and to an increase in the charge trapped in both interfaces. The maximum in $n(x)$ in the supply layer is now asymmetrical (Fig. 3) because of optical absorption, and reaches

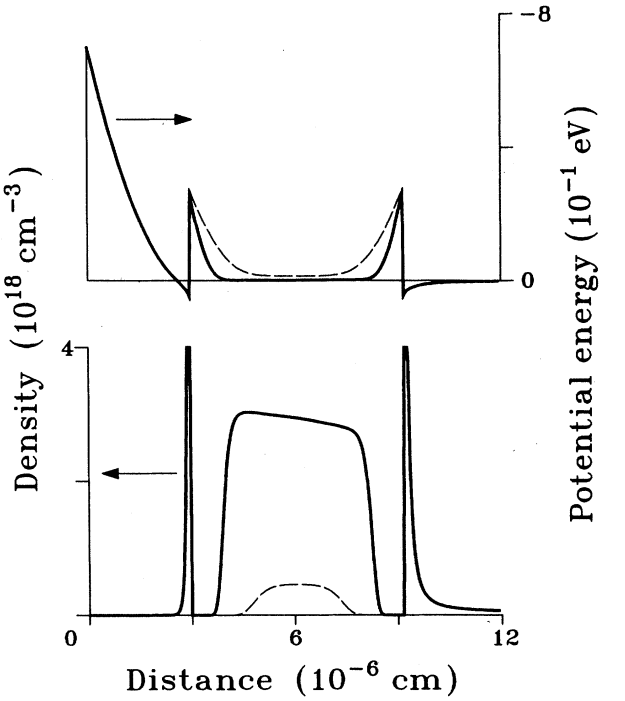

FIG. 3. Free-electron density $n(x)$ and the potential energy $\phi(x)+\Delta\phi(x)$, derived from Eq. (2), vs distance below the illuminated surface of the heterostructure of Fig. 1 at 77 K in the "dark" (dashed lines) or "light" (solid lines) condition. Outside the $Al_{0.3}Ga_{0.7}As$ layer the dashed curve differs little from the solid one and is omitted for clarity. The sharp peaks in $n(x)$ are truncated by the range of the ordinate. The optical absorption coefficient is 5×10^5 cm^{-1}, and "light" corresponds to $\sim1.5\times10^{17}$ photons s^{-1} cm^{-2} at 660 nm.

$\sim3\times10^{18}$ cm^{-3} close to the cap/$Al_{0.3}Ga_{0.7}As$ interface, where for these particular circumstances the illumination is strong enough to ionize practically all the deep donors in the supply layer. Changes in the interfacial charges cannot be shown well on the scale of Fig. 3 and are omitted for clarity, but we return to this point in Sec. IV B.

Figure 4 shows the donor contributions that constitute the electron distributions $n(x)$ of Fig. 3. In Fig. 4(a) we reproduce the $n(x)$ of Fig. 3 for comparison with the corresponding $n_d^+(x)$ and $n_s^+(x)$ in Figs. 4(b) and 4(c), respectively. In the dark the density of ionized deep donors is effectively zero throughout the structure and $n(x)$ then just reflects $n_s^+(x)$. In the illuminated case, the depletion region in the $Al_{0.3}Ga_{0.7}As$ layer just under the cap extends from $x=0.030$ μm to $\simeq0.035$ μm, and $n_d^+=3\times10^{18}$ cm^{-3} there. For increasing x beyond the depletion region, $n_d^+(x)$ is at first close to 3×10^{18} cm^{-3}, since the light ionizes practically all the deep donors there, but it falls with increasing x due to the absorption. This trend is reversed at $x\simeq0.085$ μm by the depletion of the deep donors caused by the $Al_{0.3}Ga_{0.7}As$/buffer interface, where again n_d^+ reaches 3×10^{18} cm^{-3}. Continuing into the buffer, n_d^+ is first influenced by the $Al_{0.3}Ga_{0.7}As$/buffer interface but then reaches $\sim6.3\times10^{16}$ cm^{-3} at $x=0.12$ μm.

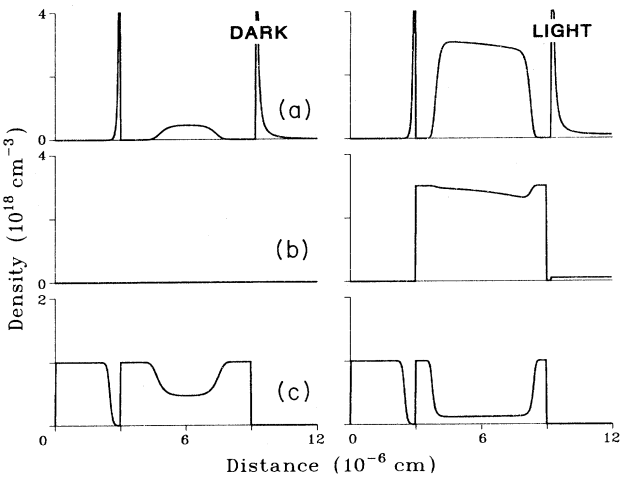

FIG. 4. Relationship of the densities of the ionized deep and shallow donors to that of free electrons for the cases of Fig. 3: (a) repeats $n(x)$ of Fig. 3 for comparison with (b) the corresponding $n_d^+(x)$ of Eq. (4), and (c) the $n_s^+(x)$ of Eq. (5). The temperature is 77 K. The sharp peaks in (a) are truncated by the range of the ordinate.

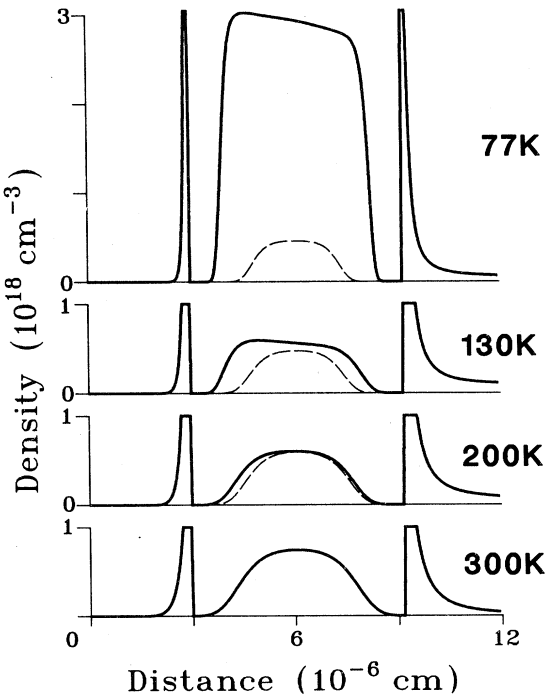

FIG. 5. Temperature dependence of the distribution of free-electron density, $n(x)$ of Eq. (2), for "dark" (dashed curves) or "light" (solid curves) conditions. Outside the $Al_{0.3}Ga_{0.7}As$ layer the dashed curves are practically indistinguishable from the solid ones on this scale and are omitted for clarity; for 300 K the curves are essentially the same even in the $Al_{0.3}Ga_{0.7}As$ layer.

The effect of light on $n_s^+(x)$ [Fig. 4(c)] follows from our implicit assumption that the shallow donors are in thermal equilibrium with the conduction bands. So when photoexcited electrons are added to the conduction bands, the shallow donors are filled correspondingly. Hence the inverse relationship between the total free-electron density of Fig. 4(a) and n_s^+ of Fig. 4(c).

B. Effect of light at different temperatures

The aim is to illustrate the experimental result[12] that the response to a steady illumination increases as temperature is reduced from 300 K. Qualitatively, this is attributed[10,13,15,16] to the inhibition of recombination through the deep donor at low temperatures. This leads to an increase in the density of photoexcited electrons in the conduction bands. Here we imitate this result and show how the distribution of the photoexcited electrons, and the density of their ionized donors, varies with temperature.

Figure 5 shows for different temperatures the distribution of the free-electron density $n(x)$ in the structure. For increasing temperature, $n(x)$ in the dark varies relatively little, but in the light it shows a marked change from 77 to 200 K as the illuminated result approaches the dark one and the effect of absorption becomes less pronounced. At 300 K the light and dark behaviors are indistinguishable on the scale of Fig. 5.

The behavior seen in Fig. 5 comes from the temperature dependence of the deep donor's contribution,[26] which is shown in Fig. 6. At 77 K $n_d^+(x)$ has the shape described in Sec. IV A. As the temperature is increased to 130 K, the influence of the depletion regions is retained close to the interfaces, and the effect of absorption is perceptible, but n_d^+ in the undepleted $Al_{0.3}Ga_{0.7}As$ drops to $\sim 1\times 10^{17}$ cm^{-3}. This decrease continues with increasing temperature and eventually it practically eliminates the depletion regions at 300 K; n_d^+ in the middle of the $Al_{0.3}Ga_{0.7}As$ layer is $\simeq 1.7\times 10^{14}$ cm^{-3} at 300 K.

In terms of the qualitative interpretations[10,13,15,16] referred to above—that the temperature dependence of the response comes from that of the recombination through the deep donors—one expects the behavior in Fig. 6 to derive from the temperature dependence of R. The reasoning is that as recombination is reduced it effectively increases the emission rate $\delta\epsilon_n$, and so increases R. Thus R should increase with reducing temperature, and this dependence should be the controlling factor behind the behavior in Fig. 6.

Inspection of Eqs. (4) and (6) confirms this for a slice taken in, say, the middle of the undepleted $Al_{0.3}Ga_{0.7}As$ layer, but shows that other factors are influential in regions affected by the interfaces. To see this, we recall that the temperature dependence of n_d^+ is contained in the factor $z_d y$, which involves three exponential terms: $\exp[-\beta(E_\Gamma-\mu_c)]$, $\exp(\beta E_{\Gamma d})$, and $\exp(\beta E_{Ld})$. They all increase with decreasing temperature because of their dependence on β and the first two tend to decrease n_d^+ through Eq. (4). However, this tendency is more than offset by the third term, $\exp(\beta E_{Ld})$, which changes relatively more than the other two. It tends to increase R [Eq. (6)] and so leads to an increase of n_d^+ through the factor g_d/R.

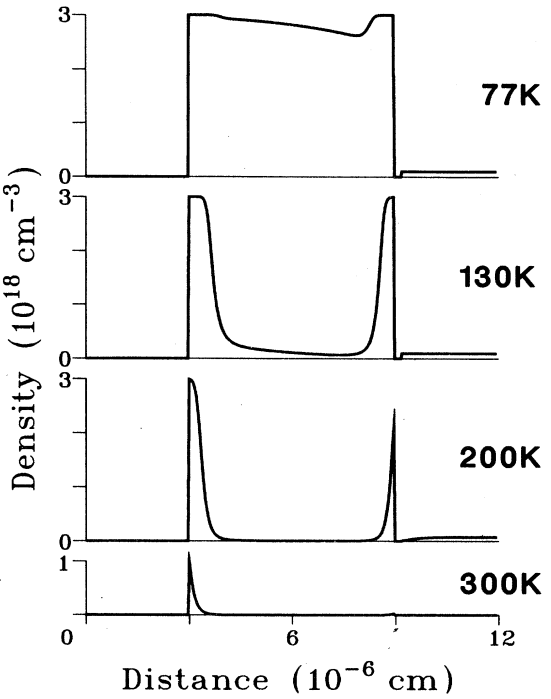

FIG. 6. As in Fig. 5, except here for the density of ionized deep donors $n_d^+(x)$ for the "light" condition. The plateaus in these curves are intrinsic and are not limited by the range of the ordinate.

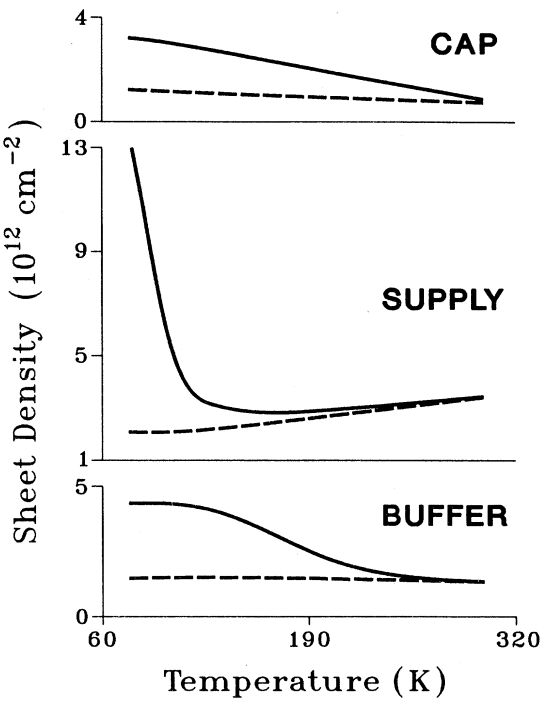

FIG. 7. Temperature dependence of the effective sheet electron density for the active layers of Fig. 1 for the "dark" (dashed curves) or "light" (solid curves) condition.

The direction of the temperature dependence of n_d^+ for a given position x in the $Al_{0.3}Ga_{0.7}As$ layer is thus determined by the variation of R, in accordance with the qualitative view mentioned above. But the magnitude of this dependence is modulated by the factor $\exp[-\beta(E_\Gamma-\mu_c)]$, which varies strongly with x. In the supply layer $E_\Gamma-\mu_c$ is largest in the depletion regions close to the interfaces (Fig. 3). Consequently, $z_d y$ is small there, and n_d^+ is relatively independent of temperature, as seen in Fig. 6. So the behavior of $n_d^+(x)$, and ultimately that of $n(x)$ in Fig. 5, derives from the interplay of these temperature-dependent and position-dependent factors in $z_d y$.

Finally, we turn to the temperature dependence of the interfacial charges. These are reflected in Fig. 7, which shows the effective sheet charge density for the principal layers obtained by trapezoidal integration of $n(x)$ in the dark or light conditions. The behavior in the supply layer is just another view of that seen in Fig. 5, and is directly comparable with experimental results obtained[10–12] for samples of supply layer materials in steady illumination (cf., for example, Fig. 5 of Ref. 12). The behavior in the cap or buffer represents essentially that of the interfacial charge, since it dominates the integration. The difference between the dark and light behaviors in these layers reflects the smooth increase in the trapped interfacial charge derived from the photoexcited electrons in the supply layer.

We note that in the dark the interfacial charge in the cap or buffer decreases with increasing temperature, as reported elsewhere,[15,27] whereas that in the supply layer increases. This follows from the sign of the argument in the exponent of Eq. (2). It is negative in the supply layer (because of the sign of $\phi+\Delta\phi$; Fig. 3) and the exponential term in Eq. (2) varies relatively little with temperature. Then the temperature dependence of n follows that of D, which increases with temperature. In the interfacial regions, however, the argument in the exponent of Eq. (2) is positive and the domination of this term reverses the influence of D. Thus in the interfaces n decreases with increasing temperature.

V. CONCLUSIONS

Using a model heterostructure and solving the 1D Poisson equation that is expanded to account for photoexcitable donors in given layers of the structure, we have derived a picture of the effect of temperature on the response of the structure to light. Our calculations cover the range 77–300 K. We have shown how the model imitates experimental results for the temperature dependences of the electron density in the active layers of a structure, and we have expanded this with a view of the distribution of this charge within the structure.

We see our approach as a first step towards a more quantitative understanding of the effect of illumination on the electrical properties of HEMT structures. It shows how the photoexcited carriers are distributed in the model structure, but the addition of such charge to the system also alters the internal potential barriers which, in the normal configuration we have considered,

control access to the different conduction channels for electrons passing between the source and the drain. Thus illumination not only increases the free-electron density, it also alters the current distribution in the device. This redistribution must be accounted for before a full assessment can be made of the effect of temperature and illumination on the electrical properties, and discussion of this aspect will be given in a future report.

ACKNOWLEDGMENT

We thank W. R. McKinnon for his continuous interest and for critically reading the manuscript.

APPENDIX

We use a standard method[28] to solve simultaneously Eqs. (1) and (2). The aim is to reduce an error p in Eq. (2) to an acceptable value using the linearizing approximation[24]

$$\exp(\Phi+p)\simeq(1+p)\exp(\Phi) . \tag{A1}$$

Here $\Phi\equiv\beta(\phi+\Delta\phi)$ of Eq. (2). The calculation proceeds in equal increments along the x axis. Let the size of the increment be h, which is small relative to the thickness of the layers in the structure, then if Φ is exact Eq. (1) can be expressed in its central difference form at the jth step as

$$\Phi_{j-1}-2\Phi_j+\Phi_{j+1}=-Q[N_j^+-n(x_j)] , \tag{A2}$$

where $Q\equiv qh^2/\epsilon_s$. But if the potential we use at the jth step is in error by p_j, so that the exact value of the potential there is (Φ_j-p_j), then substitution into Eq. (A2), combined with Eq. (A1), leads to

$$p_{j+1}+B_jp_j+p_{j-1}=D_j , \tag{A3}$$

where

$$B_j=-2-Qn(x_j) ,$$

$$D_j=\Phi_{j-1}-2\Phi_j-\Phi_{j+1}+Q[N_j^+-n(x_j)] .$$

Since Φ has given values at the top and bottom of the structure,[25] the error is zero for the first and last increments. Consequently, the error at the jth increment is given by

$$p_j=(D_j-p_{j+1})/D_j \tag{A4}$$

and Eq. (A3) reduces to iterative formulas

$$B_j^*=B_j-1/B_{j-1} ,$$

$$D_j^*=D_j-D_{j-1}/B_{j-1} ,$$

for the "new" values B^* and D^* derived from the "old." The calculation procedes by evaluating from Eq. (A4) the error for each increment, comparing the largest of these values with a preset criterion, and, through the iterative formulas, repeating this procedure until the criterion is met.

[1]M. S. Shur, *GaAs Devices and Circuits* (Plenum, New York, 1987), Chap. 10.
[2]C. S. Chang, H. R. Fetterman, D. Ni, E. Sovero, B. Mathur, and W. J. Ho, Appl. Phys. Lett. **51**, 2233 (1987).
[3]M. Heuken, L. Loreck, K. Heime, K. Ploog, W. Schlapp, and G. Weimann, IEEE Trans. Electron Devices **ED-33**, 693 (1986).
[4]T. J. Drummond, R. J. Fischer, W. K. Kopp, H. Morkoç, K. Lee, and M. S. Shur, IEEE Trans. Electron Devices **ED-30**, 1806 (1983).
[5]T. J. Drummond, W. Kopp, R. Fischer, H. Morkoç, R. E. Thorne, and A. Y. Cho, J. Appl. Phys. **53**, 1238 (1982).
[6]A. Kastalsky and J. C. M. Hwang, Appl. Phys. Lett. **44**, 333 (1984).
[7]A. Kastalsky and J. C. M. Hwang, Solid State Commun. **51**, 317 (1984).
[8]T. N. Theis and S. L. Wright, Appl. Phys. Lett. **48**, 1374 (1986).
[9]S. J. Lee and C. R. Crowell, Solid State Electron. **28**, 659 (1985).
[10]N. Chand, T. Henderson, J. Klem, W. T. Masselink, R. Fischer, Y-C. Chang, and H. Morkoç, Phys. Rev. **30**, 4481 (1984).
[11]R. J. Nelson, Appl. Phys. Lett. **48**, 351 (1977).
[12]C. M. Hurd, S. P. McAlister, W. R. McKinnon, B. R. Stewart, D. J. Day, P. Mandeville, and A. J. SpringThorpe, J. Appl. Phys. **63**, 4706 (1988).
[13]A. K. Saxena, Solid State Electron. **25**, 127 (1982).
[14]S. M. Sze, *Physics of Semiconductor Devices* (Wiley, New York, 1981).
[15]W. R. McKinnon and C. M. Hurd, J. Appl. Phys. **61**, 2250 (1987).
[16]C. E. Falt, C. M. Hurd, S. P. McAlister, W. R. McKinnon, D. J. Day, and A. J. SpringThorpe, Semicond. Sci. Technol. **2**, 513 (1987).
[17]H. J. Lee, L. Y. Juravel, J. C. Woolley, and A. J. SpringThorpe, Phys. Rev. **21**, 659 (1980).
[18]J. C. M. Henning, J. P. M. Ansems, and P. J. Roksnoer, J. Phys. C **19**, L335, (1986).
[19]H. C. Casey and M. B. Panish, *Heterostructure Lasers, Part A: Fundamental Principles* (Academic, New York, 1978), p. 192.
[20]F. M. Vorobkalo, K. D. Glinchuk, and V. F. Kovalenko, Phys. Tekh. Poluprovodn. **9**, 998 (1975) [Sov. Phys.—Semicond. **9**, 656 (1975)].
[21]K. Park and K. D. Kwack, IEEE Trans. Electron Devices **ED-33**, 673 (1986).
[22]D. E. Aspnes, S. M. Kelso, R. A. Logan, and R. Bhat, J. Appl. Phys. **60**, 754 (1986).
[23]C. M. Hurd, S. P. McAlister, D. J. Day, and J. Sitch, J. Appl. Phys. **64**, 5225 (1988).
[24]H. K. Gummel, IEEE Trans. Electron Devices **ED-11**, 455 (1964); D. L. Scharfetter and H. K. Gummel, *ibid.* **ED-16**, 64 (1969).
[25]We set ϕ at the top surface to -0.7 eV, the free-surface value

for GaAs, and assume it does not change with illumination. At the other limit, the underside of the buffer where no light penetrates, we set $\phi=(1/\beta)\ln[n(x)/D]$.

[26]It seems unnecessary to show n_s^+ in a separate figure since its behavior mirrors $n(x)$, and can therefore be judged directly from Fig. 5.

[27]K. Lee, M. Shur, T. J. Drummond, and H. Morkoç, J. Appl. Phys. **54**, 2093 (1983).

[28]Kindly provided by J. Sitch of Bell-Northern Research Labs.